

**Influence of the surface chemistry on the electric-field control of the magnetization of ultrathin films**N. Tournier,<sup>\*</sup> A. P. Engelhardt,<sup>†</sup> F. Maroun,<sup>‡</sup> and P. Allongue*Physique de la Matière Condensée, Ecole Polytechnique, CNRS, 91128 Palaiseau, France*

(Received 12 April 2012; published 28 September 2012)

In this paper we investigate the voltage dependence of magnetization anisotropy on electrodeposited Co/Au(111) ultrathin films using *in situ* real-time polar magneto-optical Kerr effect. A systematic voltage and thickness-dependent study is conducted, demonstrating that the magnetoelectric effects arise from an electric field-induced change in the surface anisotropy. The effect is linear, reversible, and can be as large as 50%. We also show that its amplitude depends on the surface chemistry of the Co films. Another kind of magnetoelectric is also reported and discussed that allows a reversible and complete spin reorientation transition in a 5.6-monolayer-thick layer covered with carbon monoxide.

DOI: [10.1103/PhysRevB.86.104434](https://doi.org/10.1103/PhysRevB.86.104434)

PACS number(s): 75.85.+t, 75.30.Gw, 78.20.Ls, 82.40.-g

**I. INTRODUCTION**

Spintronics is primarily based on the precise control of a nanostructure magnetization direction, which stability over time and magnetic addressing are becoming increasingly important issues in device miniaturization. One line of research is tailoring the magnetic anisotropy energy (MAE) of the nanostructure, e.g., by using ordered alloys such as L1<sub>0</sub> FePt<sup>1</sup> or superlattices Co/Pt<sup>2</sup> and Co/Pd.<sup>3</sup> A second line of research aims at manipulating the magnetization of nanostructures<sup>3-5</sup> by injecting a spin-polarized current,<sup>6</sup> or more recently, by applying a voltage.<sup>7-16</sup> The latter method is particularly appealing as it would allow reducing device power consumption, since direct current is not necessary.

Since the pioneering paper of Weisheit *et al.*,<sup>9</sup> the electric field is thought to be the origin of a voltage-induced magnetoelectric effect (ME). They exploited the large electric field existing at the solid/electrolyte contact but nevertheless measured nonlinear ME of a few percent only, which they assigned to changes of the electron band filling inside the *whole* CoPd or FePt layer, although the electric field is screened over less than one atomic plane at metal electrodes.<sup>17</sup> Zhernenkov *et al.*<sup>12</sup> also used an electrochemical (EC) contact to investigate CoPd thin films by means of polarized neutron reflectivity and concluded that changes in magnetization spread over 7.2 nm. However, the solid/electrolyte interface structure was clearly ill defined with the presence of an oxide and an organic layers. All other groups working in this area employed a solid dielectric layer to separate the magnetic film from the second contact. Generally, a very thin MgO layer is first deposited on the magnetic film (FeCo,<sup>10</sup> Fe,<sup>11,15</sup> and also Co<sup>13</sup>) before a leakage-free high-*k* oxide thin film and an metal contact are deposited. The top contact can also be just an ionic liquid layer deposited on the MgO film.<sup>18,19</sup> A common behavior in these studies is the *asymmetry* of the ME upon potential bias sign and the ME reversibility. Namely, with a few exceptions, the ME is large at a positive gate voltage only and is very small at a negative gate voltage. Bauer *et al.*<sup>15</sup> assigned this behavior to charge trapping in the oxide layer. A systematic study of ME with applied voltage was also missing, probably because of the very long time constant to reach a steady state.

Convincing experimental evidence is, therefore, still missing to unambiguously quantify the voltage-induced ME, to determine its dependence on the surface chemistry of the

magnetic film, and to determine whether ME stems from the surface or the bulk. This last question of highest scientific importance is only debated in a number of theoretical papers, which consider self-standing layers<sup>20,21</sup> or more realistic systems.<sup>22,23</sup> Experimentally, the challenge is avoiding the shortcomings associated with the deposition of the dielectric layer. The EC interface, where the magnetic film is in contact with an electrolyte, is an appealing solution<sup>24</sup> when high-purity chemicals are being used. The EC interface corresponds to an ideal electric contact, where charges in the metal and the first ionic plane in the solution are separated by a monolayer (ML) of water molecules. Thus, macroscopically uniform large electric fields (>1 V/nm) may be easily obtained, allowing a quantitative study of the ME. Moreover, this “soft” contact does not generate any structural defects in the magnetic film.

In this paper we investigate the voltage dependence of magnetization anisotropy on electrodeposited Co/Au(111) ultrathin films using *in situ* real-time polar magneto-optical Kerr effect (PMOKE). A systematic voltage and thickness-dependent study is conducted demonstrating that the MEs arise from an electric field-induced change in the surface anisotropy. The effect is linear, reversible, and can be as large as 50%. We also show that its amplitude depends on the surface chemistry of the Co films. Another kind of ME is also reported and discussed that allows a reversible and complete spin reorientation transition (SRT) in a 5.6-ML-thick layer covered with carbon monoxide.

**II. EXPERIMENTAL METHODS**

Epitaxial ultrathin Co(0001) layers were grown electrochemically as reported in Refs. 25 and 26 on ~8-nm-thick Au(111) epitaxial buffer layers electrochemically deposited on Si(111).<sup>27</sup> The MEs were investigated by installing the sample in an EC flow cell, equipped with an optical window, placed onto a home-built PMOKE setup for recording in real-time magnetization curves *M-H* as a function of potential. A Pt wire is used as a counterelectrode and a saturated mercury/mercury sulfate electrode (MSE) as a reference of potentials. In all magnetoelectric experiments presented below, the Co layers are deposited at a potential of -1.3 V, and deposition is stopped by applying  $U \sim -1.15$  V (no cobalt deposition or dissolution occurs at this potential). Then, Co<sup>2+</sup> ions were removed by circulating a Co<sup>2+</sup> free electrolyte so that no cobalt

deposition takes place during ME experiments. The plating solution was 0.1 M  $K_2SO_4$  + 1 mM  $KCl$  + 1 mM  $H_2SO_4$  + 1 mM  $CoSO_4$  (pH  $\sim$  4). All solutions were prepared with reagent grade chemicals using Milli-Q water (resistivity of 18.2  $M\Omega cm$ ). In all ME experiments shown below, the sample reflectivity was also measured *in situ* (sensitivity 0.1 ML) to check that the deposit did not undergo dissolution.

### III. RESULTS AND DISCUSSION

Past *in situ* magnetic studies in our group showed that as-grown electrodeposited Co/Au(111) films undergo a SRT around 1.6 ML,<sup>28</sup> meaning that they are out-of-plane magnetized below  $\sim$ 1.6 ML and in-plane magnetized above. This critical thickness is smaller than 4 ML, the value measured in ultrahigh vacuum (UHV),<sup>29</sup> indicating a significantly weaker surface anisotropy energy. We assign this difference to the H-termination of the Co surface in the EC environment.<sup>30</sup> The H-coverage is nearly potential independent below  $-1$  V.<sup>31</sup>

Figure 1 presents  $M$ - $H$  curves of a 1.7-ML-thick film recorded at  $-1.15$  V (open circles) and  $-1.6$  V (filled symbols). The  $M$ - $H$  curve becomes remarkably squarer when the applied potential is made more negative. The effect is completely reversible as two curves recorded at the same potential in subsequent potential sweeps perfectly overlap (Fig. 1, lines). The variation of the coercive field ( $H_C$ ) as a function of potential is perfectly linear (Fig. 1, inset) with a slope  $\Delta H_C/\Delta U = -217$  Oe  $V^{-1}$ , much larger than reported previously.<sup>9</sup> From the ratio between remanant and saturation magnetizations one obtains  $M_R/M_S \sim 0.91$  (respectively 0.61) at  $-1.6$  V (respectively  $-1.15$  V) yielding an easy axis relative tilt of  $27^\circ$ . This is quite a significant rotation angle. Above 2 ML (in-plane magnetized films), the ME was monitored by determining the magnetic susceptibility  $\chi$  [ $\chi = \Delta M/\Delta H$ , the slope of  $M$ - $H$  curve; see inset of Fig. 2(a)] as a function of the potential. Figure 2(a) shows that  $\chi$  varies linearly (negative slope) with the potential for all Co thicknesses ( $t_{Co}$ ). The effect is again reversible (negative- and positive-going potential sweeps perfectly overlap), and it is again quite large ( $\sim$ 40–50% per volt). Since  $\chi$  varies linearly

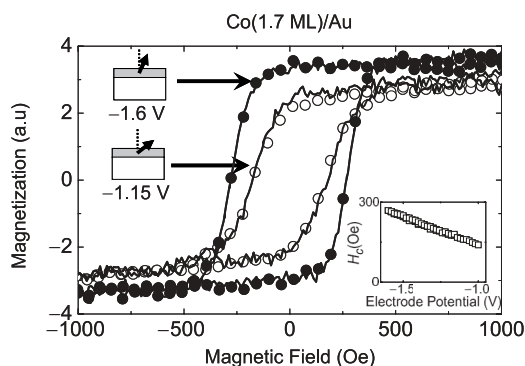


FIG. 1.  $M$ - $H$  curves of 1.7 ML Co film at  $-1.6$  V (filled circles) and  $-1.15$  V (open circles). The same curves are measured at either potential upon successive potential ramps (solid lines). Drawings indicate the orientation of the magnetization easy axis for each  $M$ - $H$  curve. Inset: plot of the coercive field as a function of potential (slope =  $-217$  Oe  $V^{-1}$ ).

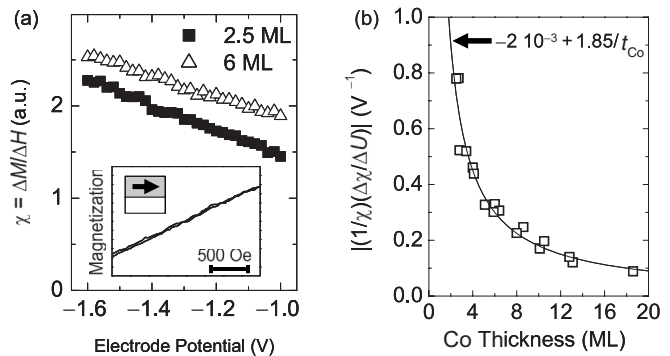


FIG. 2. (a) Plots of the magnetic susceptibility  $\chi$  of 2.5- and 6-ML Co films as a function of potential. Inset: typical  $M$ - $H$  curve for Co films thicker than 2 ML. (b) Relative susceptibility  $|(1/\chi)(\Delta\chi/\Delta U)|$  per volt as a function of the Co film thickness for films with in-plane magnetization easy axis. The solid line is the best fit by the  $C_1/t_{Co} + C_2$  law ( $C_1 = 1.85$  and  $C_2 = -2 \cdot 10^{-3}$ ).

with the potential, the absolute value of  $(1/\chi)(\Delta\chi/\Delta U)$  is a representative parameter, and it allows comparing films of different thicknesses. Figure 2(b) shows that  $|(1/\chi)(\Delta\chi/\Delta U)|$  decays rapidly as  $C_1/t_{Co} + C_2$  [see best fit in Fig. 2(b)].

Figure 2(b) shows a first indication that the magnetolectric effect stems essentially from the surface. The thickness dependence,  $C_1/t_{Co} + C_2$ , may actually be analytically derived from standard models based on the minimization of the sum of the different anisotropy energies (dipolar, magnetocrystalline, interface, and Zeeman).<sup>32</sup> In the case of a film with a magnetization easy axis not strictly out-of-plane, the master equation is

$$K_1 - 2\pi M_{sat}^2 + K_S/t_{Co} + 2K_2(\sin\theta)^2 + HM_{sat}/(2\cos\theta) = 0, \quad (1)$$

where  $t_{Co}$  is the average cobalt thickness,  $\theta$  the angle between the magnetization easy axis and the surface normal,  $M_{sat}$  the absolute magnetization at saturation ( $1407$  emu  $cm^{-3}$  for bulk cobalt), and  $K_S$  the interface anisotropy constant, which decomposes into two terms  $K_S = (K_S^{Surf} + K_S^{Co-Au})$ ,  $K_S^{Co-Au} \sim 0.5$  erg. $cm^{-2}$  being the surface anisotropy of the Co/Au interface, and  $K_S^{Surf}$  that of the Co/electrolyte interface.  $K_1 \sim 5.6 \cdot 10^6$  erg  $cm^{-3}$  and  $K_2 \sim 1.6 \cdot 10^6$  erg  $cm^{-3}$  are bulk magnetocrystalline anisotropy constants of hcp Co(0001).<sup>25</sup> For Co films thicker than 2 ML and an applied field  $H$  small with respect to the Co saturation field ( $\sim 10^4$  Oe),  $\theta$  is close to  $\pi/2$  and  $\sin\theta \sim 1$ . Since the PMOKE signal  $M$  is  $M = \alpha M_{sat} \cos\theta$ ,  $\alpha$  being a proportionality coefficient, one may write using Eq. (1)

$$M \approx \frac{\alpha H}{2} \frac{M_{sat}^2}{2\pi M_{sat}^2 - K_1 - 2K_2 - K_S/t_{Co}} = H\chi. \quad (2)$$

For Co films thicker than 2 ML,  $K_S/t_{Co}$  is small with respect to  $K_V$ , the sum of the volume anisotropies ( $K_V = 2\pi M_{sat}^2 - K_1 - 2K_2 = 3.6 \cdot 10^6$  erg  $\cdot$   $cm^{-2}$  in the case of Co). Consequently,  $(1/\chi)(\Delta\chi/\Delta U)$  is in a first-order

approximation in  $(1/K_V)(K_S/t_{Co})$

$$\begin{aligned} \frac{1}{\chi} \frac{\Delta\chi}{\Delta U} \approx & \frac{2}{M_{sat}} \frac{\Delta M_{sat}}{\Delta U} \left[ 1 - \frac{2\pi M_{sat}^2}{K_V} \left( 1 + \frac{K_S}{K_V} \frac{1}{t_{Co}} \right) \right] \\ & - \frac{1}{K_V} \frac{\Delta(K_1 + 2K_2)}{\Delta U} \left( 1 + \frac{K_S}{K_V} \frac{1}{t_{Co}} \right) \\ & + \frac{1}{K_S} \frac{\Delta K_S}{\Delta U} \left( \frac{K_S}{K_V} \frac{1}{t_{Co}} \right), \end{aligned} \quad (3)$$

assuming that all quantities depend on  $U$ . The best fit of data in Fig. 2(b) with a  $C_1/t_{Co} + C_2$  law (solid line in the figure) yields  $C_1 = 1.85 \pm 0.1 \text{ V}^{-1}$  and  $C_2 = -2.10^{-3} \pm 0.02 \text{ V}^{-1}$ . In spite of the fitting error,  $C_2$  is negligibly small with respect to the values of  $(1/\chi)(\Delta\chi/\Delta U)$ , demonstrating that the dominant change in Eq. (3) upon varying the potential is that of  $K_S$  and that the ME is a *pure* surface effect. In addition, because of the metallic nature of Co and Au, the potential drop is significant at the Co/electrolyte only. Thus, we can conclude that the magneto-optic effect is due to the Co/electrolyte interface, i.e.,  $K_S^{\text{Surf}}$ . The value  $C_1 = 1.85 \text{ V}^{-1}$  yields  $\Delta K_S^{\text{Surf-H}}/\Delta U = -0.13 \text{ erg cm}^{-2} \text{ V}^{-1}$ , which is rather large (the H superscript in the expression of  $\Delta K_S$  corresponding to the hydrogen termination of the Co surface in the present experiments). In the case in which films present a remnant magnetization, it is easy to establish the relation between  $\Delta K_S^{\text{Surf}}/\Delta U$  and  $M_R/M_S$  using Eq. (1) with  $H = 0$  and recalling that  $M_R/M_S = \cos\theta$ :

$$\frac{\Delta K_S^{\text{Surf}}}{\Delta U} = 2K_2 t_{Co} \frac{\Delta[(M_R/M_S)^2]}{\Delta U}. \quad (4)$$

The analysis of  $M$ - $H$  curves in Fig. 1 yields  $K_S^{\text{Surf-H}} = -0.415-0.133 U$  in  $\text{erg cm}^{-2}$  with  $U$  in volts with respect to the MSE. The two determinations of  $\Delta K_S^{\text{Surf-H}}/\Delta U$  are in close agreement, which supports the validity of both analyses. The primary conclusion of this work is therefore that the ME is linear and reversible with the potential (negative slope) and is a pure field effect. In addition its thickness dependence demonstrates that it is a pure surface effect. These conclusions have not yet been clearly established experimentally for the reasons given in the Introduction. Our conclusion is in agreement with recent calculations,<sup>21</sup> even though the predicted sign and amplitude are still under debate in the case of Co.<sup>20</sup> Last, the above voltage dependence  $\Delta K_S^{\text{Surf}}/\Delta U$  is among the highest ever reported. Reported values are smaller by a factor of 10 to 100 at solid contacts. A direct comparison between EC and solid-state contacts is, however, made difficult because of the uncertainty in determining the electric field in the latter case.

To further investigate the ME on perpendicularly magnetized layers and for a different surface termination, we adsorbed CO on an as-prepared Co layer. This was done by the circulation of a CO-saturated electrolyte after depositing the Co film. CO adsorption increases the MAE layer as it keeps the film perpendicularly magnetized up to a Co thickness  $\sim 6$  ML, yielding at  $-1.15 \text{ V}$   $K_S^{\text{Surf-CO}} = +0.16 \text{ erg cm}^{-2}$  ( $K_S^{\text{Surf-H}} = -0.26 \text{ erg cm}^{-2}$ ). The MAE obtained here at room temperature is similar to that reported in the case of Co/Pd(111) layers in UHV below 200 K.<sup>33</sup> According to literature, CO adsorption displaces the initially present H-monolayer on metals, and the CO coverage is potential independent in the potential range investigated here. Figure 3(a) shows that a 4-ML CO-dosed Co/Au(111) film

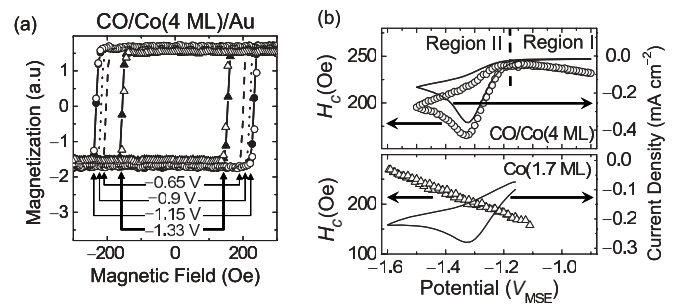


FIG. 3. (a)  $M$ - $H$  curves of a CO-dosed 4-ML Co film at  $-1.33$ ,  $-1.15$ ,  $-0.9$ , and  $-0.65 \text{ V}$ , extracted from a series recorded during two potential sweeps. Closed symbols belong to first sweep and the open ones to the second sweep. (b) Upper panel line, the EC current associated with the reduction of  $\text{H}^+$  into  $\text{H}_2$  at the CO-covered Co/Au(111) layer. Upper panel, open circles:  $H_C$  as a function of potential. Note the close correlation of  $H_C$  with the EC current for  $U < -1.15 \text{ V}$  (Region II). Lower panel line: the EC current associated with the reduction of  $\text{H}^+$  into  $\text{H}_2$  on as-grown Co/Au(111) layer. Lower panel, open triangles:  $H_C$  as a function of potential. Note that  $H_C$  and the EC current are completely uncorrelated in this case.

is perpendicularly magnetized over the whole investigated potential range. However, close inspection of the figure reveals two regimes of variations as  $H_C$  first *increases* between  $-0.9$  and  $-1.15 \text{ V}$  before it strongly *decreases* at  $-1.33 \text{ V}$ . Again, these variations are reversible. To highlight the differences between the two regimes of variations, Fig. 3(b) presents the potential dependence of  $H_C$  [Fig. 3(b), higher panel, open circles] together with the current-potential curve [Fig. 3(b), higher panel, line]. In Region I ( $-1.18 \text{ V} < U < -0.9 \text{ V}$ ),  $H_C$  varies *linearly* and reversibly with the applied potential as in the case of H-terminated Co film. This is clear proof that an electric field effect is also occurring at the CO-covered surface. Region I is also characterized by the absence of any EC current [Fig. 3(b), top panel]. Analyzing the  $M$ - $H$  curves of CO-covered Co films of thickness close to  $\sim 6$  ML, we obtain  $K_S^{\text{Surf-CO}} = -0.12-0.24 U$ . The magnitude of the effect (absolute value of  $\Delta K_S^{\text{Surf-CO}}/\Delta U$ ) is larger than at the H-terminated surface. In Region II ( $U < -1.15 \text{ V}$ ),  $H_C$  behavior is completely different.  $H_C$  becomes nearly proportional to the EC current with a slope  $-240 \text{ Oe cm}^2 \text{ mA}^{-1}$ . This behavior is also reversible and is observed after removing dissolved CO from the solution, indicating that the CO coverage of the Co surface is not altered during the potential cycle. We also emphasize that this behavior is specific of the CO-terminated surface as it is not observed in the case of H-covered Co films. For comparison, Fig. 3(b), lower panel, shows the variations of  $H_C$  (open triangles) and the EC current (line) for a 1.7-ML H-covered Co layer. Despite a similar EC current,  $H_C$  remains linear with the potential and not correlated with the electrochemical current.

The electrochemical current flowing for  $U < -1.18 \text{ V}$  corresponds to the hydrogen evolution reaction (HER) where  $\text{H}^+$  is transformed into  $\text{H}_2$  gas. HER involves the formation of  $\text{H}_{\text{ads}}$  reaction intermediate,<sup>31</sup> which is not considered as the HER limiting step. Thus,  $\text{H}_{\text{ads}}$  coverage is nearly independent of the applied potential on an as-grown Co film.

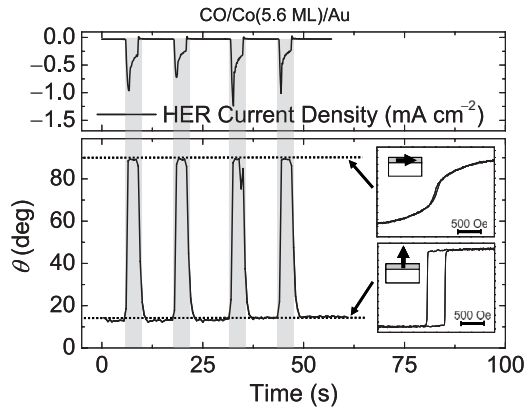


FIG. 4. Influence of the HER current (upper panel) on the magnetization easy axis angle  $\theta$  (with respect to the film normal) for a 5.6-ML CO-covered Co film (lower panel) as a function of time during four consecutive potential steps between  $-1.15$  V and  $-1.3$  V or  $-1.4$  V. The two  $M$ - $H$  curves in the inset of the lower panel correspond to a HER current of  $\sim 0$   $\text{mA cm}^{-2}$  (lower curve) and  $< -0.4$   $\text{mA cm}^{-2}$  (upper curve). Notice the reversibility of the process for the successive potential steps.

At the CO-covered surface, the mechanism of HER is not documented. However, since the CO layer is not desorbed during HER, we tentatively infer that the reaction forces the formation of the  $\text{H}_{\text{ads}}$  species on the surface sites not occupied by CO molecules. Contrary to the bare surface, the HER limiting step in this case is most probably the formation of  $\text{H}_{\text{ads}}$  on the CO-covered surface.  $\text{H}_{\text{ads}}$  coverage is thus expected to increase with increasing EC current density  $I$ . Consequently, the change in MAE seems to be related to the  $\text{H}_{\text{ads}}$  coverage.

The surface anisotropy energy during HER ( $K_S^{\text{Surf-CO-HER}}$ ) contains, within a crude approximation, two contributions  $K_S^{\text{Surf-CO}}$  and  $K_S^{\text{Surf-H}}$ , the weight of each being related to the surface coverage of adsorbed CO and  $\text{H}_{\text{ads}}$ , respectively. As  $K_S^{\text{Surf-H}} < 0$  and  $|K_S^{\text{Surf-CO}}| \sim |K_S^{\text{Surf-H}}|$ , it is straightforward that  $K_S^{\text{Surf-CO-HER}}$  may become smaller than  $K_S^{\text{Surf-CO}}$ , which explains our observations. Going beyond this simple picture necessitates precise density functional theory calculations.

Finally, we exploited this behavior to show that one can completely reorient the magnetization easy axis from out-of-plane to in-plane, at a CO-covered Co/Au(111) film of thickness 5.6 ML. Figure 4 presents the time dependence of the angle  $\theta$  between magnetization and surface normal upon application of four consecutive pulses of voltage from  $-1.15$  V (no HER) to  $-1.4$  or  $-1.5$  V (HER): in the absence of HER current (nonshaded areas), the magnetization easy axis is perpendicular, whereas it tilts by  $\theta \sim 90^\circ$  upon HER current flowing (shaded areas). This flipping of the magnetization resembles that obtained by Sander *et al.* who demonstrated reversible magnetization flipping in Ni films upon H adsorption in UHV.<sup>34</sup> However, in our case, the H coverage is controlled by the potential, and the magnetization flipping is obtained with a mixed surface chemistry H and CO. Finally, the observed magnetochemical current effect is highly interesting and should open up new routes for the magnetization manipulation of nanostructures.

In conclusion, we demonstrated that the MEs in Co ultrathin films arise from an electric field-induced change in the surface anisotropy. We also show that the effect is linear, reversible, and can be as large as 50%. In addition, its amplitude depends on the surface chemistry of the Co films. We also reported on another kind of ME that allows a reversible and complete SRT in a 5.6-ML-thick layer covered with carbon monoxide

\*Present address: Laboratoire Matériaux et Génie Industriel, ECAM Rennes–Louis de Broglie, Campus de Ker Lann, 35091 Rennes, France; nicolas.tournerie@ecam-rennes.fr

†Present address: Computational Electronics and Photonics Group, Electrical Engineering Department and Center for Interdisciplinary Nanostructure Science and Technology, University of Kassel, Wilhelmshöher Allee 71, 34121 Kassel, Germany; andreas.engelhardt@uni-kassel.de

‡Corresponding author: fouad.maroun@polytechnique.fr

<sup>1</sup>J. Lee, C. Brombacher, J. Fidler, B. Dymerska, D. Suess, and M. Albrecht, *Appl. Phys. Lett.* **99**, 062505 (2011).

<sup>2</sup>H. Bernas, T. Devolder, C. Chappert, J. Ferre, V. Kottler, Y. Chen, C. Vieu, J. P. Jamet, V. Mathet, E. Cambril, O. Kaitasov, S. Lemerle, F. Rousseaux, and H. Launois, *Nucl. Instrum. Methods Phys. Res., Sect. B* **148**, 872 (1999).

<sup>3</sup>D. Litvinov, V. Parekh, E. Chunsheng, D. Smith, J. O. Rantschler, P. Ruchhoeft, D. Weller, and S. Khizroev, *IEEE Trans. Nanotechnol.* **7**, 463 (2008).

<sup>4</sup>H. J. Richter, A. Y. Dobin, R. T. Lynch, D. Weller, R. M. Brockie, O. Heinonen, K. Z. Gao, J. Xue, R. J. Veerdonk, P. Asselin, and M. F. Erden, *Appl. Phys. Lett.* **88**, 222512 (2006).

<sup>5</sup>M. K. Grobis, O. Hellwig, T. Hauet, E. Dobisz, and T. R. Albrecht, *IEEE Trans. Magn.* **47**, 6 (2011).

<sup>6</sup>C. Chappert, A. Fert, and F. N. Van Dau, *Nat. Mater.* **6**, 813 (2007).

<sup>7</sup>D. Chiba, M. Yamanouchi, F. Matsukura, and H. Ohno, *Science* **301**, 943 (2003).

<sup>8</sup>D. Chiba, M. Sawicki, Y. Nishitani, Y. Nakatani, F. Matsukura, and H. Ohno, *Nature (London)* **455**, 515 (2008).

<sup>9</sup>M. Weisheit, S. Fähler, A. Marty, Y. Souche, C. Poinignon, and D. Givord, *Science* **315**, 349 (2007).

<sup>10</sup>Y. Shiota, T. Maruyama, T. Nozaki, T. Shinjo, M. Shiraishi, and Y. Suzuki, *Appl. Phys. Express* **2**, 063001 (2009).

<sup>11</sup>T. Maruyama, Y. Shiota, T. Nozaki, K. Ohta, N. Toda, M. Mizuguchi, A. A. Tulapurkar, T. Shinjo, M. Shiraishi, S. Mizukami, Y. Ando, and Y. Suzuki, *Nat. Nanotechnol.* **4**, 158 (2009).

<sup>12</sup>M. Zhernenkov, M. R. Fitzsimmons, J. Chlistunoff, J. Majewski, I. Tudosa, and E. E. Fullerton, *Phys. Rev. B* **82**, 024420 (2010).

<sup>13</sup>D. Chiba, S. Fukami, K. Shimamura, N. Ishiwata, K. Kobayashi, and T. Ono, *Nat. Mater.* **10**, 853 (2011).

<sup>14</sup>Y. Shiota, T. Nozaki, F. d. r. Bonell, S. Murakami, T. Shinjo, and Y. Suzuki, *Nat. Mater.* **11**, 39 (2012).

<sup>15</sup>U. Bauer, M. Przybylski, J. r. Kirschner, and G. S. D. Beach, *Nano Lett.* **12**, 1437 (2012).

- <sup>16</sup>U. Bauer, S. Emori, and G. S. D. Beach, *Appl. Phys. Lett.* **100**, 192408 (2012).
- <sup>17</sup>A. J. Bard and L. R. Faulkner, *Electrochemical Methods: Fundamentals and Applications* (John Wiley and Sons, New York, 2001).
- <sup>18</sup>M. Kawaguchi, K. Shimamura, S. Ono, S. Fukami, F. Matsukura, H. Ohno, D. Chiba, and T. Ono, *Appl. Phys. Express* **5**, 063007 (2012).
- <sup>19</sup>K. Shimamura, D. Chiba, S. Ono, S. Fukami, N. Ishiwata, M. Kawaguchi, K. Kobayashi, and T. Ono, *Appl. Phys. Lett.* **100**, 122402 (2012).
- <sup>20</sup>K. Nakamura, R. Shimabukuro, Y. Fujiwara, T. Akiyama, T. Ito, and A. J. Freeman, *Phys. Rev. Lett.* **102**, 187201 (2009).
- <sup>21</sup>Chun-Gang Duan, Julian P. Velev, R. F. Sabirianov, Ziqiang Zhu, Junhao Chu, S. S. Jaswal, and E. Y. Tsymbal, *Phys. Rev. Lett.* **101**, 137201 (2008).
- <sup>22</sup>S. Subkow and M. Fahnle, *Phys. Rev. B* **84**, 054443 (2011).
- <sup>23</sup>K. Nakamura, T. Akiyama, T. Ito, M. Weinert, and A. J. Freeman, *Phys. Rev. B* **81**, 220409 (2010).
- <sup>24</sup>W. Schindler and J. Kirschner, *Phys. Rev. B* **55**, R1989 (1997).
- <sup>25</sup>L. Cagnon, T. Devolder, R. Cortes, A. Morrone, J. E. Schmidt, C. Chappert, and P. Allongue, *Phys. Rev. B* **63**, 104419 (2001).
- <sup>26</sup>P. Allongue, L. Cagnon, C. Gomes, A. Gundel, and V. Costa, *Surf. Sci.* **557**, 41 (2004).
- <sup>27</sup>P. Prod'homme, F. Maroun, R. Cortes, and P. Allongue, *Appl. Phys. Lett.* **93**, 171901 (2008).
- <sup>28</sup>P. Allongue, F. Maroun, H. F. Jurca, N. Tournerie, G. Savidand, and R. Cortes, *Surf. Sci.* **603**, 1831 (2009).
- <sup>29</sup>G. Rodary, V. Repain, R. L. Stamps, Y. Girard, S. Rohart, A. Tejada, and S. Rousset, *Phys. Rev. B* **75**, 184415 (2007).
- <sup>30</sup>J. H. Hafner, C. L. Cheung, T. H. Oosterkamp, and C. M. Lieber, *J. Phys. Chem. B* **105**, 743 (2001).
- <sup>31</sup>J. O. M. Bockris, B. E. Conway, and E. Yeager, *Comprehensive Treatise of Electrochemistry*, Vol. 2 (Plenum Press, New York, 1980).
- <sup>32</sup>M. T. Johnson, P. J. H. Bloemen, F. J. A. d. Broeder, and J. J. d. Vries, *Rep. Prog. Phys.* **59**, 1409 (1996).
- <sup>33</sup>D. Matsumura, K. Amemiya, S. Kitagawa, T. Shimada, H. Abe, T. Ohta, H. Watanabe, and T. Yokoyama, *Phys. Rev. B* **73**, 174423 (2006).
- <sup>34</sup>D. Sander, W. Pan, S. Ouazi, J. Kirschner, W. Meyer, M. Krause, S. Muller, L. Hammer, and K. Heinz, *Phys. Rev. Lett.* **93**, 247203 (2004).